Infrared luminescence and application of a vibronic-coupling Hamiltonian to the level structure of CdTe:Fe^{2+}

E. E. Vogel and O. Mualin
Departamento de Ciencias Físicas, Universidad de La Frontera, Casilla 54-D, Temuco, Chile

M. A. de Orúe, J. Rivera-Iratchet, and M. L. Flores
Departamento de Física, Universidad de Concepción, Casilla 4009, Concepción, Chile

U. W. Pohl
Institut für Festkörperphysik, Technische Universität Berlin, Hardenbergstrasse 36, D-10623 Berlin, Germany

H.-J. Schulz and M. Thiede
Fritz-Haber-Institut der Max-Planck-Gesellschaft, Faradayweg 4-6, D-14195 Berlin, Germany
(Received 25 January 1994)

Samples of crystalline CdTe doped with two different concentrations of iron were prepared by the vertical high-pressure Bridgman method. Absorption and emission spectra were recorded at liquid-helium temperature in the region of the $^5T_2(D) \rightleftharpoons {}^5E(D)$ infrared transitions of substitutional $Fe^{2+}(d^6)$ ions. Especially in the range between 2200 and 2300 cm^{-1}, a rich structure is resolved comprising more lines than predicted from plain crystal-field theory. The explanation of all the important lines is found after introducing a vibronic Jahn-Teller term to the Hamiltonian. A linear coupling between the double-degenerate vibrational mode ϵ (or γ_3) to the electronic orbitals of the atomic multiplet of symmetry ^5D leads to the diagonalization of the total Hamiltonian in a set of vibronic functions. Just one free parameter is used in the adjustment: the so-called Jahn-Teller energy representing the strength of the coupling. The corresponding value that we report here is 3 cm^{-1}. The energies thus found are in good agreement with the positions of the observed lines in the spectra. With the final wave functions we can calculate the relative intensities of the most important transitions and approximate theoretical line shape. This is also in good agreement with the experiment. Using these same energies and wave functions a calculation was performed to explain data existing in the literature about far-infrared absorption for the system CdTe:Fe^{2+}. Again, good agreement between experiment and theory is found.

I. INTRODUCTION

The usual ionization state of substitutional Fe in zinc-blende compounds is Fe^{2+} which corresponds to a ^5D atomic multiplet. The tetrahedral crystalline field on a cation site splits these 25 states into an excited $^5T_2$ level and the ground level ^5E. We use the notation corresponding to the irreducible representations of point group T_d to label the states and wave functions. (The equivalent greek-letter notation will be preferred for vibronic states.) Spin-orbit interaction further splits these levels, producing a scheme such as the one presented on the left-hand side of Fig. 1.[1,2] Both crystal-field and spin-orbit interactions cause admixture with other excited atomic multiplets; this influence is not explicitly shown in the energy-level diagram.

We discuss below the low-temperature luminescent transitions originating from the T_2 level, the lowest one in the excited multiplet. The electric-dipole operator transforms as the irreducible representation T_2 (or Γ_5 from now on) of T_d. Then, the allowed transitions should lead to levels in the low multiplet with symmetries contained in the reduction of the following Kronecker product:

$$T_2 \otimes \Gamma_5 \rightarrow A_1 + E + T_1 + T_2 \ . \tag{1}$$

Plain crystal-field theory predicts that the ground multiplet splits into five equally spaced levels of symmetries A_1, A_2, E, T_1, and T_2, which allow luminescent transitions to the four of them explicitly shown in Eq. (1), following selection rules for electric-dipole transitions (EDT's). For reasons to be discussed below magnetic-dipole transitions (MDT's) are weaker than EDT's but still of interest here and will be considered in our calculations. The prediction of this introductory model is a luminescent spectrum formed by four equally spaced lines.[2] They are shown as downward arrows on the left-hand side of Fig. 1, where the transitions are labeled as $L1$, $L2$, $L3$, and $L4$ in order of decreasing energies. The predicted intensities are such that $L1$, $L3$, and $L4$ are approximately of the same intensity while $L2$ should be markedly stronger (EDT only).[1,2]

The experimental information available for Fe^{2+} in III-V compounds of zinc-blende structure shows general but not total agreement with this scheme. This is the case for GaP:Fe^{2+},[3-5] GaAs:Fe^{2+},[6,7] InP:Fe^{2+},[5,7-11] and InAs:Fe^{2+}.[6] Generally speaking the main characteristics of these spectra are the following: (a) The num-

ber of important lines is four; (b) their relative intensities are such that $L2$ is much stronger than any of the other three lines that present similar intensities; (c) the lines are not equally spaced ($L2$ and $L3$ are closer than the others); (d) in some experiments an additional broad structure is found for energies less than the one corresponding to $L4$.

All of the above characteristics have been recently explained in terms of a dynamic Jahn-Teller (JT) coupling of two-dimensional vibrational modes γ_3 (or ϵ) to the electronic multiplet ^5E.[2,12] Moreover, it is predicted that the low-energy structure is due to several weak lines that become more important as the coupling frequency decreases. From this point of view, InSb would be ideal to test this prediction. However, the low-energy gap of this semiconductor makes the experimental observation nearly impossible.[2] This is one of the reasons to turn our attention in the present paper to a II-VI semiconductor like CdTe with a wider energy gap, but still presenting a lattice dynamics with abundance of low-frequency modes.[13,14]

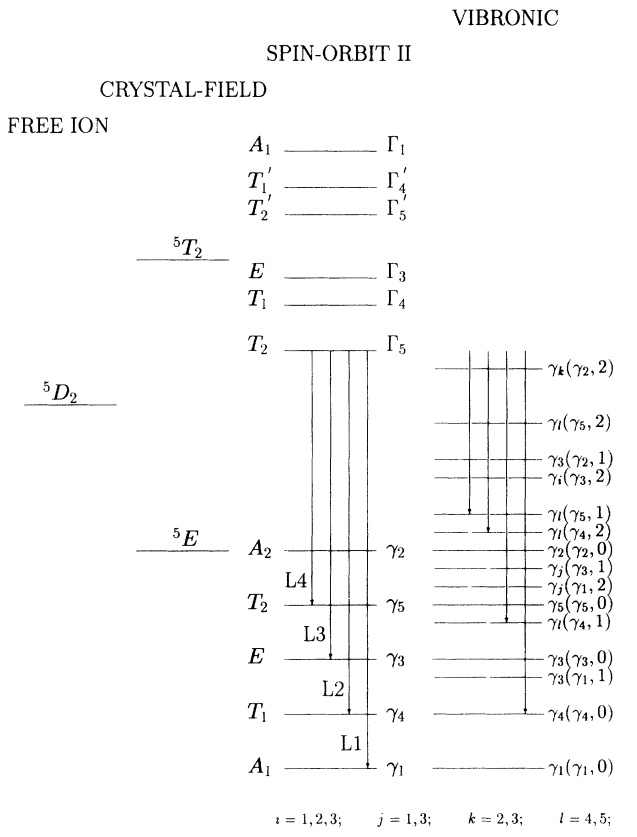

FIG. 1. Schematic of the splitting due to the crystalline field and second-order spin-orbit interaction for a d^6 system such as Fe^{2+}. Symbols for the irreducible representations of the point group T_d are used to label the electronic levels. Capital greek letters are used for the levels originating from the upper multiplet while lower-case ones are used for the lower multiplet. The arrows represent the only possible electric-dipole-luminescent transitions. When more than one transition ending in a level of the same symmetry is possible we distinguish them by means of primes, double primes, and so on, in order of decreasing energies. This is the case of the lines $L2$, $L2'$, $L2''$, and $L2'''$, shown as downward arrows in order of decreasing energy without labeling. This scheme is not to scale and represents a particular way to classify the 25 electronic functions.

A review of the literature, looking for luminescence experiments for Fe^{2+} in II-VI materials, shows that there is less information available than for the same ion in III-V compounds. This is a second reason to carry out experimental and theoretical work on CdTe. Nevertheless, we can mention that the spectra of ZnS:Fe^{2+} (Ref. 15) and ZnSe:Fe^{2+} (Refs. 16 and 17) show all four of the characteristics mentioned above. All of this points toward CdTe as the best candidate to show additional lines in the luminescence spectra of Fe^{2+} in II-VI compounds.

There is even a third reason for picking CdTe:Fe^{2+} for the present work. Far-infrared absorption measurements for this system done long ago showed more lines than expected.[18,19] Several efforts were made to explain such a rare spectrum.[18,20,21] However, the fact that all previous experimental methods failed to locate levels of symmetry E (or γ_3) rendered the theoretical interpretation uncertain. As already pointed out, the luminescent transitions will locate such levels, making it possible to explain the old absorption data along with the spectra to be reported below.

In the following section we present the main aspects of the sample preparation, equipment, and measuring techniques. Section III contains a summary of the theoretical framework that will be used here. The theoretical results are presented in Sec. IV, comparing them with the experiments and discussing the manifestation of the JT coupling in these systems. In Sec. V we revisit the data on far-infrared absorption spectra involving the same energy levels already characterized. Without any further adjustment the old data are finally explained in a satisfactory way, giving a complete and consistent picture for the low-energy-level states of CdTe:Fe^{2+}. General and particular conclusions are given in the last section.

II. EXPERIMENT AND MEASUREMENTS

A. Experimental techniques

CdTe crystals were prepared by the vertical high-pressure Bridgman method from a stoichiometric melt. Fe doping of nominal 100 and 1000 ppm was performed during growth, using elemental iron.

Luminescence and transmission spectra are recorded in a setup assembled around an evacuable Jarrell-Ash grating spectrometer. Repetitive scans are rendered possible through a stepper drive and lock-in signal processing and averaging. The samples are cooled by liquid helium in an immersion cryostat equipped with CaF_2 windows. For more details of the measurement particulars, see the captions of Figs. 2 and 3.

B. Experimental results

The emission spectrum for the less-doped sample (Fig. 2) in the range of the $^5T_2(^5D) \rightarrow {}^5E(^5D)$ transitions displays four distinct lines at 2283, 2264, 2237, and 2209

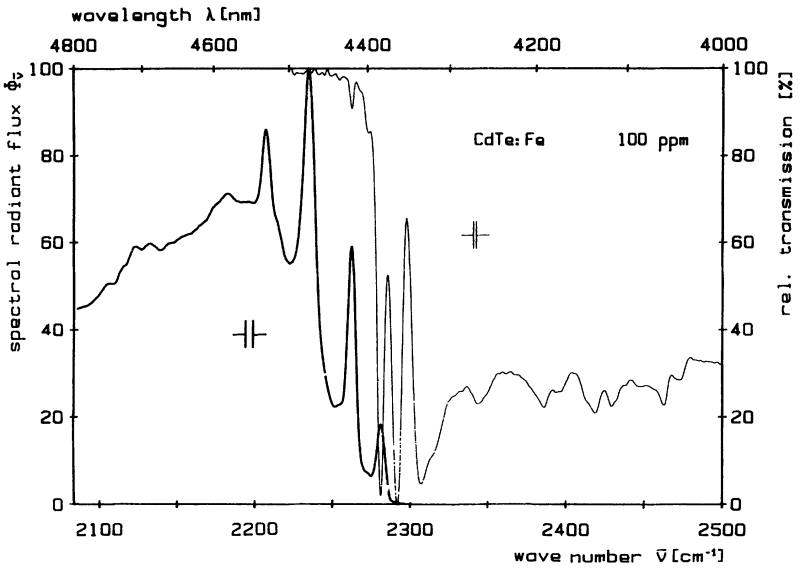

FIG. 2. Survey of the low-temperature emission (bold trace, left) and transmission (thin trace, right) of a CdTe:Fe crystal, 100-ppm Fe nominal doping, at $T \simeq 4$ K, grating blazed at $\lambda = 2.6$ μm, InSb detector (liquid-N_2 cooled). No corrections. Emission excited by Ar ion laser (1-W output) on front surface.

cm^{-1}. They are superimposed to a broad band suggesting a stronger phonon coupling than that known from II-VI compounds with a larger band gap, e.g., ZnS.[22] Although the general feature of nearly equal spacing is roughly retained, the general pattern looks quite different from, for example, the simpler spectra of Fe^{2+} in III-V compounds.[2,12] Particularly the dominance of the second line $L2$, also familiar from the spectra of the same ion in ZnS and III-V semiconductors, is lost here.

Nevertheless, this transition ($L2$ at 2264 cm^{-1}) is clearly discernible in the respective transmission spectrum (Fig. 2), which also exhibits the inverse of the first no-phonon line ($L1$ at 2283 cm^{-1}) known from luminescence. In addition, there are absorptive structures at higher energies, especially a sharp line at 2293 cm^{-1} followed by a broader structure near 2309 cm^{-1}.

A specimen doped by a higher amount of iron features all the mentioned structures with the addition of supplementary information in both emission and absorption (Fig. 3). The luminescence reveals additional peaks or shoulders at 2257, 2233, and 2217 cm^{-1} and even some weaker signals at 2294 and 2274 cm^{-1}. In the transmission data minima at 2274, 2256, and 2232 are discernible. For wave numbers $\bar{\nu} > 2310$ cm^{-1} this sample is opaque.

When the temperature is lowered to approximately 2 K (from the 4 K in the reported spectra), the absorptions near 2274 and 2264 cm^{-1} are clearly diminished, proving their origin at a level above the ground state of the Fe^{2+} center. The same reaction is expected for the 2256- and 2232-cm^{-1} absorptions but is less clearly pronounced in these instances.

Under the conditions of above-gap excitation of the front surface, the strength of $L1$ and $L2$ varies with the location of the illuminated spot on the crystal. The effect is most pronounced for $L1$, which can be increased by a factor of up to 2.5 as compared to $L3$.

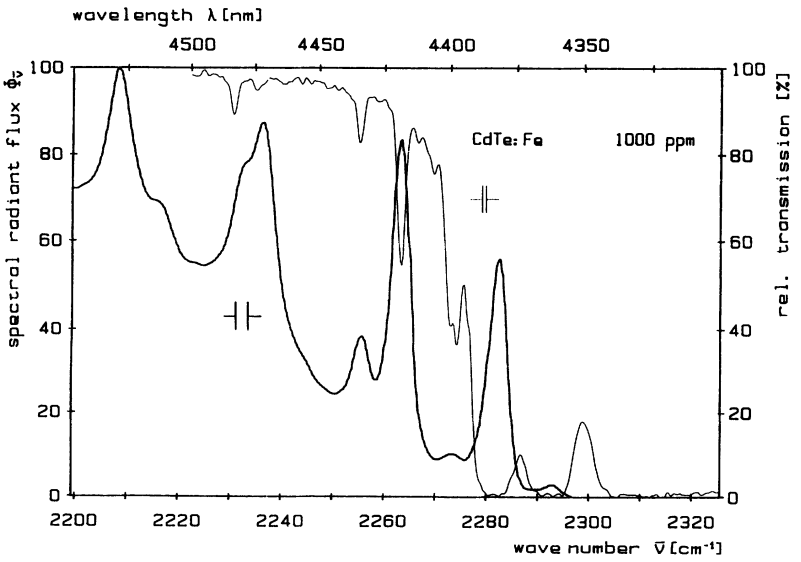

FIG. 3. Details of the low-temperature emission (bold trace) and transmission spectra (thin trace) in the no-phonon region, taken with a CdTe:Fe crystal of higher nominal doping level (1000-ppm Fe). Otherwise the same conditions as in Fig. 2 hold except for increased resolution, cf. spectral slit widths indicated.

III. THEORY

The vibronic coupling described here is basically the same as the one used to explain the luminescent spectra of Fe^{2+} in III-V compounds.[2] In the present paper we will summarize its most important aspects. The main special feature, which is the lattice dynamics of the host crystal, will be introduced after the general presentation.

Our main hypothesis is that phonons of symmetry ϵ (or γ_3) couple to the electronics levels. We are mainly interested in the coupling to those states that are final states for luminescent transitions. This means that we want to study the coupling to the five electronic components of the lower multiplet, namely, $\epsilon\otimes A_1$, $\epsilon\otimes T_1$, $\epsilon\otimes E$, $\epsilon\otimes T_2$, and $\epsilon\otimes A_2$. From the resulting couplings we look for those states that have a significant component of zero-phonon states of symmetries A_1, T_1, E, and T_2, in accordance with the selection rules for EDT's found in Eq. (1). Similarly, we also look for zero-phonon states of symmetries A_2, T_1, E, and T_2, which have the right symmetry properties for MDT's. Our starting point is the set of atomic levels, which we assume to be known. The crystalline field ($10|Dq|$) and spin-orbit interactions ($\lambda\mathbf{S}\cdot\mathbf{L}$) are then added as components of the total Hamiltonian. The vibrational Hamiltonian for the two coupling modes θ and ϵ of energy $\hbar\omega$ is given by

$$H_v=\hbar\omega(a_\theta^\dagger a_\theta+a_\epsilon^\dagger a_\epsilon+1)\ , \tag{2}$$

where the usual annihilation and creation operators a_α and $a_\alpha^\dagger$ are used ($\alpha=\theta,\epsilon$).

The coupling Hamiltonian can now be written as

$$H_{\rm JT}=\sqrt{\hbar\omega E_{\rm JT}}[(a_\theta^\dagger+a_\theta)D_\theta+(a_\epsilon^\dagger+a_\epsilon)D_\epsilon]\ , \tag{3}$$

where $E_{\rm JT}$ is the so-called Jahn-Teller energy, the only adjustable parameter in the present approach.

Crystalline parameter $10|Dq|$ is calculated by considering the first line $L1$ and remains fixed at the value 2478 cm^{-1}. The spin-orbit parameter λ is introduced with its free-ion value, -100 cm^{-1}. The coupling phonon must have a local component of symmetry ϵ at the impurity site. There are three points of the Brillouin zone that fulfill this condition. This was discussed fully for the case of $InP:Fe^{2+}$, where the conclusion was that the $TA(L)$ modes are the most important ones for the coupling in zinc-blende compounds.[2] Then, the value of $\hbar\omega$ is directly read from the lattice-dynamics literature, namely, 30 cm^{-1}.[13,14] We are left with $E_{\rm JT}$ as the only free parameter, which is now varied to obtain the best adjustment to the experimental spectra given in Figs. 2 and 3.

The vibronic wave functions will be defined in the Born-Oppenheimer limit, i.e., the weak-coupling limit ($E_{\rm JT}\to 0$) in the usual way.[23] In brief, a basis increasing to N vibrational quanta is multiplied by the electronic functions of the different levels in the ground multiplet. The larger N is, the larger the Hamiltonian matrix is, and the better the precision reached. All of this algebra is done by means of group theory. This tool helps to break the total Hamiltonian matrix into submatrices of different symmetries.

The diagonalization of the Hamiltonian will render the energies E_μ, E'_μ, E''_μ, etc., where μ is the index reflecting the symmetry properties of the vibronic function. They can be expressed as a linear combination of basis functions built in the Born-Oppenheimer limit originating from electronic functions of symmetry e ($e=1,2,3,4,5$), combined with n vibrational quanta of the chosen modes. The primes are just a practical way to label these different functions of similar symmetry.

As a way to illustrate the formation of a particular submatrix, let us consider a basis of vibronic functions of symmetry γ_1. The first trivial element of this set of functions is of electronic symmetry γ_1 ($e=1$) with zero phonon ($n=0$). Such a function is denoted $|\gamma_1(\gamma_1 0)a\rangle$. We then notice that the vibronic functions, resulting from the product of a γ_1 electronic function times one-phonon vibrational states, lead to vibronic functions of symmetry γ_3, namely, $|\gamma_3(\gamma_1 1)\alpha\rangle$ (with $\alpha=\theta,\epsilon$). The second element of the set of γ_1 functions is to be given by $|\gamma_1(\gamma_3 1)a\rangle$ ($e=3$, $n=1$). Then for two-vibrational quanta we have $|\gamma_1(\gamma_1 2)a\rangle$ ($e=1$, $n=2$) and so on. This is illustrated on the right-hand side of Fig. 1.

The general notation for the basis of vibronic functions is $|\gamma_\mu(en)f\rangle$, where we refer to the fth vibronic wave function of the γ_μ multiplet ($\mu=1,2,3,4,5$). Such a state is reached by taking the product of a γ_e electronic level ($e=1,2,3,4,5$) times the vibrational level corresponding to n vibrational quanta, namely, $\gamma_3^n(\epsilon^n)$.

The final vibronic functions after the diagonalization will be linear combinations of these basis functions. We simply refer to them as γ_μ, γ'_μ, γ''_μ, and so on, in order of increasing energy for a given symmetry μ.

We report the theoretical energies in a relative way with respect to $L1$. Namely, we introduce the energy differences

$$\Delta_\mu=E_\mu-E_1\ , \tag{4}$$

which is what will be used in the subsequent analysis. It follows that $\Delta_1=0$ and will coincide with the axis of abscissas in some figures below.

With the vibronic wave functions it is possible to calculate the oscillator strengths for the luminescent transitions. A calculation for the *absolute* oscillator strengths for both EDT and MDT is beyond the scope of this paper. It would require mixing with excited atomic levels due to the crystalline-field and spin-orbit corrections, followed by the appropriate vibronic treatment. On the other hand, MDT requires the knowledge of the electrical permittivity at the precise site of the magnetic impurity. This is not known, since the values usually reported for this parameter reflect an average value throughout the crystal.[21]

Since both the $^5T_2$ and the ^5E multiplets originate from the same atomic level they have essentially the same orbital parity; it follows that EDT's are forbidden if the admixture between atomic levels would be totally neglected. When such an admixture is considered, some small contributions with different parities will appear in the wave functions, leading to weak EDT's. This allows one to consider MDT's as competing or at least contributing slightly to the total intensity of the lines. The importance

of MDT's in this type of transition has already been introduced and studied.[20,23]

We can partially avoid the difficulties involved in the oscillator-strength calculations using *relative* oscillator strengths (ROS's) as defined in other similar calculations.[23] This will be handled in a separate way for EDT's and MDT's. Anyhow, we should point out that the analysis based on the intensity of the lines is less precise than the one based on the energy differences of the observed lines. On top of the theoretical difficulties dealing with the admixture of excited atomic orbitals, there are also experimental difficulties. We have already pointed out that the relative intensities vary with the point of the sample actually exposed to the exciting radiation. We will not pursue this aspect of the problem now.

So we attempt just a general discussion concerning the intensity of the lines, seeking just to complement and illustrate the precise analysis based on the position of the lines. What we do is to calculate the angular integrals of the oscillator strengths for all possible transitions, assuming that the orbital admixture is common for all the symmetries. Of course this is a crude approximation but it is a working assumption. Still those transitions that are forbidden from the angular part will remain so. EDT's and MDT's are plotted in independent arbitrary units, so relative intensities apply separately for each set of transitions. Actually we will never mix EDT's and MDT's for actual numerical comparison.

The total Hamiltonian is now exactly diagonalized in the set of vibronic wave functions defined with up to N phonons. This process is performed for given values of E_{JT}, which are varied within a broad interval (roughly, $0 \leq E_{JT} \leq \hbar\omega$ in the first approach). Eventually a value of E_{JT} is found that yields energies that agree with the observed lines. Our proposal for the right value of the free parameter ($E_{JT}=3$ cm^{-1}) is shown by a vertical line in Fig. 4. The horizontal short bold lines in this figure indicate the vibronic levels leading to the most important calculated emissions. The corresponding symmetries of these particular energy levels are explicitly shown in Fig. 4.

The next step is to make sure that our Hamiltonian matrix is large enough to give precise and stable results that will not vary noticeably as we go to the matrix with $N+1$ phonons. Our criterion of stability is that the predicted energy difference between $L1$ and $L2$ does not vary in more than 1% as we go to the next matrix.[24] Such an analysis was indeed performed for all of the most relevant low-energy levels for $E_{JT}=3$ cm^{-1}. It was found that for $N=3$ we find stability for all levels. We shall use $N=6$ for even better precision.

After the energies are adjusted we are left with a set of final vibronic wave functions that can be used to calculate ROS's for EDT's and MDT's. We want to stress that such calculations do not imply any further variation of parameters or adjustment.

It is found that several transitions, allowed from the group-theoretical point of view, are too weak to be noticed in the experiment. That is the case of the level originated from $\gamma_1(\gamma_1,2)$ in the weak-coupling limit, which would have an intensity for EDT's of about 0.02 with respect to that of $L1$, so this level is not marked as an accessible energy level in Fig. 4. We include in our analysis all intensities for EDT's of at least one-tenth that for $L1$.

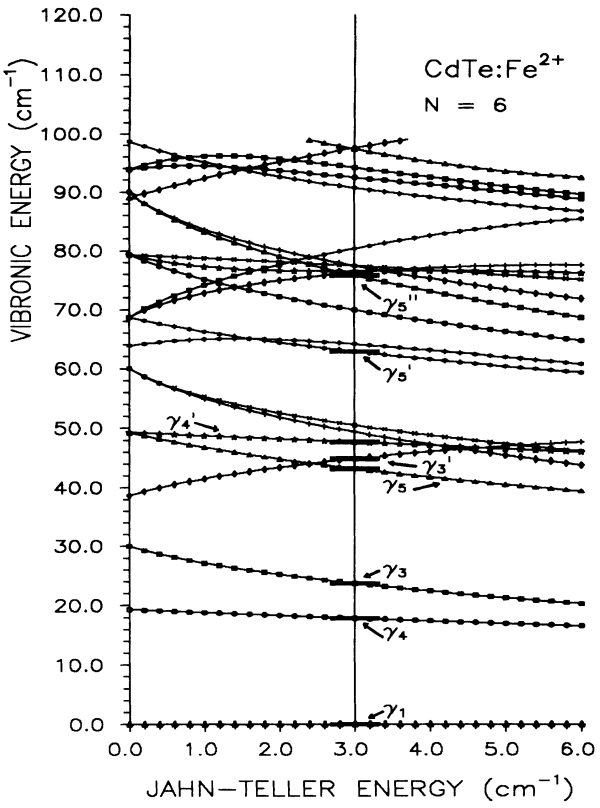

FIG. 4. Schematic of the low-energy levels as a function of E_{JT}, truncated at 100 cm^{-1}. When E_{JT} takes the value 3.0 cm^{-1} (marked as a vertical line) the positions of several vibronic levels show good correspondence with observed lines. Moreover, with the corresponding wave functions the intensities of the lines can be calculated. Short and bold horizontal lines mark the most important lines as expected from the theoretical calculations in the text. The symmetry of these eight relevant lines is also presented. Clearly correspondence to experiment is possible and unique.

IV. DISCUSSION

The crystals grown as discussed above present a well-defined although complex spectrum as presented in Figs. 2 and 3. The more important lines are now compared with the calculated transitions.

The first aspect to compare is the number of observed lines with respect to the number of predicted lines. Then it follows the actual energies of the energy levels and its comparison with the observed lines. At last we can perform a qualitative comparison dealing with the intensities of the lines.

From Fig. 2 we learn that the most important transitions lead to energy differences of 0, 19, 46, and 74 cm^{-1}. They correspond quite well to the lines at 0, 18, 45, and 76 cm^{-1}, which can be read from Fig. 4. When impurity concentration is increased new emissions are seen at ener-

gy differences of 26, 50, and 66 cm^{-1}, as shown in Fig. 3. They correspond to the theoretical lines at 24, 48, and 64 cm^{-1} reported in Fig. 4.

In the second spectrum, there are two very weak lines that are not accounted for in our theoretical model; they correspond to energy differences of -11 and 9 cm^{-1}, respectively. The second one might well be at least partially an overlap of the two leading lines due to the heavier doping. The extremely weak line at 2294 cm^{-1} has no clear explanation. A possible hypothesis is impurity-impurity interaction, which would be supported by the absence of this line in the more dilute sample. If this is so, then the line at 2274 cm^{-1} could also originate from this mechanism combined with the already mentioned overlap.

On the other hand, the theoretical results of Fig. 4 predict a line for $\Delta_5 \simeq 43$ cm^{-1} with a rather weak ROS (0.10 for EDT only). Such a line will be practically swept under the line $\Delta_3' \simeq 45$, which has a larger ROS (0.76 for EDT only). With the same train of thought, the theoretical line for $\Delta_4' \simeq 48$ with a ROS of 0.19 (EDT only) and a slightly wider separation could show as a shoulder to the low-energy region of the spectrum. This can be readily seen in the experimental results presented in Fig. 3.

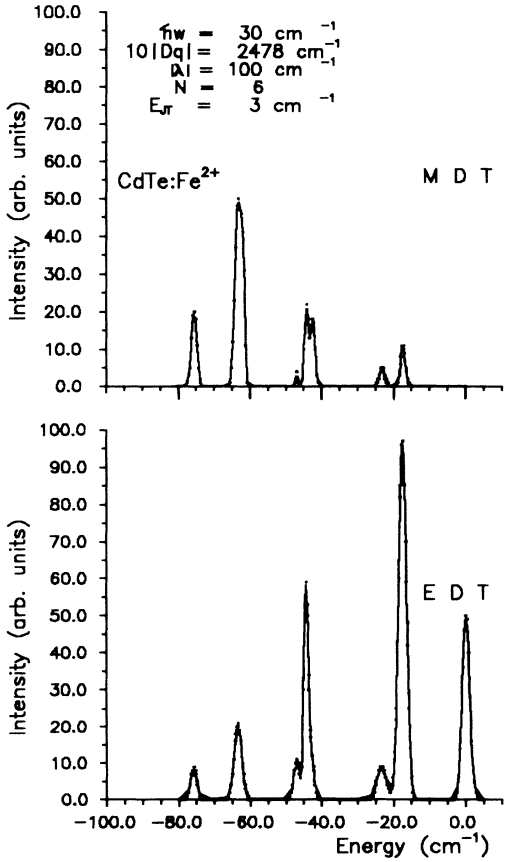

FIG. 5. Calculated line shapes of the luminescent spectrum considering electric-dipole transitions (lower part) and magnetic-dipole transitions (upper part). There is no implication of the relative importance of one component with respect to the other one. However, in the text it is shown that electric-dipole transitions remain as the dominant mechanism. No phononic background is considered.

A more general picture of the theoretical results is obtained when ROS's are fed into a Gaussian line-shape analysis. The result of this treatment is presented in Fig. 5, where arbitrary linewidths have been introduced to resemble the luminescent experimental spectrum. The lower part of this curve corresponds to EDT while the upper part of the curve corresponds to MDT, as discussed above.

The general agreement between experiment and theory (EDT) is quite clear. The importance of MDT's could be seen from the fact that they contribute very little to $L2$, while there is an important contribution to the lower-energy emissions. This can explain the appearance of the spectrum where $L2$ is not strongly dominant as in other cases.[2] Nevertheless, the main characteristics of the emission spectra can be accounted for by EDT only, which means that MDT is noticed only in the regions of the spectrum where EDT is absent or very weak.

V. APPLICATIONS TO FAR-INFRARED ABSORPTION

With the same energies and wave functions calculated above we can attempt to explain the existing data on far-infrared absorption spectra for $CdTe:Fe^{2+}$.[18,20,21] At this point there is no variation of any parameter since the levels are precisely the same as those involved in the luminescent spectrum. The absorptions originate from the true ground state γ_1 as shown on the left-hand side of Fig. 6 (which has been taken from Fig. 4 at $E_{JT}=3$ cm^{-1}).

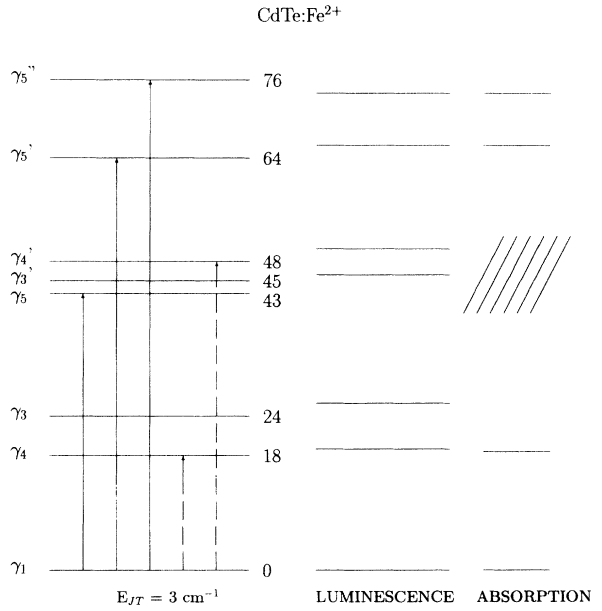

FIG. 6. On the left-hand side we present a schematic of the eight levels showing an important zero-phonon component as already stressed in Fig. 4. Then, in the central part we draw the positions of the main luminescent lines in our experiment as taken from Fig. 3. Finally, we reproduce the positions of the main absorption lines for $CdTe:Fe^{2+}$ as taken from Ref. 19; oblique lines represent a region of absorption where it is difficult to single out any individual line.

By similar arguments as those already discussed above, EDT would lead to absorptions ending on a vibronic function of symmetry γ_5 only (continuous arrows in Fig. 6). By the same token, MDT's lead to absorptions involving vibronic functions of symmetry γ_4 only (discontinuous arrows in Fig. 6). In the far-infrared region of the spectrum, it is enough to consider vibronic levels originating from the lower multiplet ^5E.

The left-hand side of Fig. 6 reproduces to scale the energy levels as already found in Sec. IV, indicating symmetry and the actual values of energy in units of cm^{-1}. We use primes, double primes, etc., to distinguish vibronic functions of the same symmetry in order of increasing energy. In the central part of this figure we present the main energy of those levels reported by our luminescent spectra as discussed above, using the same energy scale. On the right-hand side of this same figure we present the energies of the low-temperature far-infrared absorptions (LTFIA's) as taken from the literature.[19]

The first reported LTFIA, at about 18.6 cm^{-1}, is in good correspondence with the line at 19 cm^{-1} experimentally reported and at 18 cm^{-1} theoretically calculated above. This is clear manifestation of a MDT in these systems. It is then necessary to consider them either as an isolated line (as in this case) or as additional contributions to existent lines due to EDT.

The second energy level was observed at 26 cm^{-1} and calculated at 24 cm^{-1}. However, LTFIA would not show this level due to selection rules that inhibit both EDT and MDT to vibronic levels of total symmetry γ_3.

The following candidates for LTFIA are γ_5 (EDT) and γ_4' (MDT). It turns out that the wave function corresponding to γ_5 presents a tremendous admixture, lowering the possible intensities of transitions to it (as already noticed when we tried to explain the luminescent data). On the other hand, γ_4' is also a mixed state, which leads to a weak MDT. This is one reason the experiment is not very conclusive in this portion of the spectrum. Another element to be considered is the presence of several high-temperature absorptions in the same range of energies. Even at low temperatures they cannot be completely suppressed, thus masking the precise position of energy level γ_4'. We represent this inaccuracy by means of a set of oblique bars on the right-hand side of Fig. 6.

The last two LTFIA's at 66 and 74 cm^{-1} coincide precisely with our experiment above and are in reasonable agreement with our calculated γ_5' and γ_5'' at 64 and 76 cm^{-1}, respectively.

The best way to report the calculated absorptions is by means of a Gaussian line-shape analysis as we did for luminescence. In Fig. 7 we present our calculated spectrum (without the phononic background). The lower part of this figure corresponds to EDT, while the upper part of it corresponds to MDT. We must say that EDT's and MDT's are plotted in independent arbitrary units, so relative intensities apply separately for each set of transitions. Actually we will never mix EDT's and MDT's for actual numerical comparison. Arbitrary linewidths have been introduced, to resemble the experimental spectrum.

The general agreement of both sources of experimental data with our theoretical model developed above is quite remarkable indeed. Moreover, our luminescent experiment reported above yields information about the levels of symmetry γ_3 not realized so far.

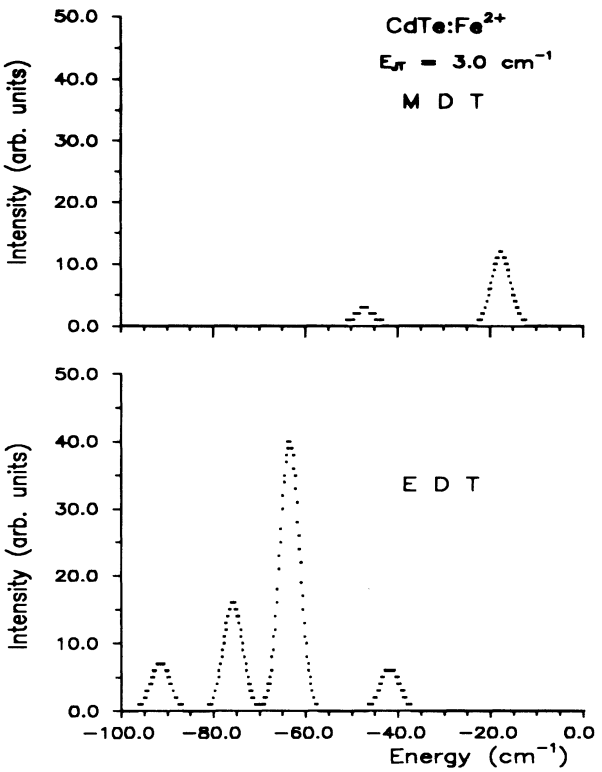

FIG. 7. Calculated line shapes of the far-infrared absorption spectrum considering electric-dipole transitions (lower part) and magnetic-dipole transitions (upper part). There is no implication of the relative importance of one component with respect to the other one. Clearly, magnetic-dipole transitions are playing a small but significant role. Otherwise the absorption at 19 cm^{-1} would not be observable.

Most of the analysis above has been concerned with the emission spectrum in order to compare it with the predictions of the theoretical model presented above. Now, we briefly turn our attention to the transmission spectrum presented by the weaker line in Fig. 2. The main characteristics of it are the three absorption lines around 2300 cm^{-1}. Our measurements show close resemblance to a rather recent experiment for the same kind of system.[25] In the explanation of this result the authors claim a C_{3V} distortion on top of the ideal T_d crystal-field symmetry. However, an interpretation also can be reached by assuming a Jahn-Teller coupling to the electronic levels of the upper multiplet.[23]

VI. CONCLUSIONS

The experiments reveal numerous discernible transitions indicative of vibronic coupling in the fine structure of levels originating from the ^5D multiplet corresponding to a $Fe^{2+}(d^6)$ configuration. They are better understood when grouped around a coinciding leading zero-phonon transition ($L1$) that plays the role of an energy reference.

While the general features in the spectra are well developed for crystals doped with 100 ppm, some of the structural details are much clearly pronounced for the higher doping level employed, i.e., 1000 ppm.

The theoretical model presented above, along with the computational algorithms that follow it, allow a good description of the vibronic coupling near a magnetic impurity, like the system under consideration.

The energy levels that follow from the interpretation of the luminescent spectrum fit well with the existing data on far-infrared low-temperature absorption. The theoretical model provides a good background for the quantitative interpretation of both spectra. Namely, we propose that a Jahn-Teller coupling of phonons of E symmetry, with a vibrational quantum $\hbar\omega = 30\ \mathrm{cm}^{-1}$ [corresponding to the TA(L) modes of the lattice dynamics] is responsible for this effect. The vibronic coupling can be characterized by means of the so-called Jahn-Teller energy, which in our case is given by $E_{\mathrm{JT}} = 3.0\ \mathrm{cm}^{-1}$.

Some minor differences between theory and experiments in the position of a few levels (less than 2 cm^{-1}, in any case) are of no importance. Let us consider that with a linear JT Hamiltonian, with only one kind of coupling mode and varying just one parameter (E_{JT}), we could predict the number of observed lines, their energies, and approximate intensities for two different experiments.

The system CdTe:Fe^{2+} shows a behavior that is different from the same ion in ZnS, ZnSe,[15–17,22] and the whole family of III-V compounds.[2] It is not known what kind of behavior the intermediate system ZnTe:Fe^{2+} will show. We are planning to perform the luminescent experiment followed by the same theoretical treatment in the future.

ACKNOWLEDGMENTS

It is a pleasure to acknowledge support by both the German Ministry of Research and Technology granted through the Stabsabteilung Internationale Beziehungen in Kernforschungszentrum Karlsruhe, and the Program of International Scientific Cooperation of Fundación Andes-CONICYT (Chile). The first five authors also acknowledge FONDECYT (Chile) under Grant No. 1930385, Dirección de Investigación y Desarrollo of Universidad de la Frontera, and Dirección de Investigación of Universidad de Concepción for partial support.

[1] G. A. Slack, F. S. Ham, and R. M. Chrenko, Phys. Rev. **152**, 376 (1966).

[2] E. E. Vogel, O. Mualin, M. A. de Orúe, and J. Rivera-Iratchet, Phys. Rev. B **44**, 1579 (1991).

[3] C. L. West, W. Hayes, J. F. Ryan, and P. J. Dean, J. Phys. C **13**, 5631 (1980).

[4] B. V. Shanabrook, P. B. Klein, and S. G. Bishop, Physica B **116**, 444 (1983).

[5] A. Louati, T. Benyattou, P. Roura, G. Bremond, G. Guillot, and R. Coquille, Mater. Sci. Forum **38-41**, 935 (1989).

[6] P. B. Klein, S. G. Bishop, R. L. Henry, A. M. Kriman, and N. D. Wisley, Mater. Sci. Forum **10-12**, 1117 (1986).

[7] P. Leyral, C. Charreaux, and G. Guillot, J. Lumin. **40-41**, 329 (1988).

[8] W. H. Koschel, U. Kaufmann, and S. G. Bishop, Solid State Commun. **21**, 1069 (1977).

[9] S. G. Bishop, P. B. Klein, R. L. Henry, and B. D. McCombe, in *Proceedings of the Conference on Semi-Insulating III-V Materials, Nottingham, 1980,* edited by G. J. Rees (Shiva, Orpington, England, 1981), p. 161.

[10] P. Leyral, G. Bremond, A. Nouailhat, and G. Guillot, J. Lumin. **24-25**, 245 (1981).

[11] K. Thonke, K. Pressel, H. U. Hermann, and A. Dornen, Mater. Sci. Forum **38-41**, 869 (1989).

[12] E. E. Vogel, O. Mualin, M. A. de Orúe, and J. Rivera-Iratchet, Phys. Rev. B **49**, 2907 (1993).

[13] J. M. Rowe, R. M. Nicklow, D. L. Price, and K. Zanio, Phys. Rev. B **10**, 671 (1974).

[14] H.-Matsuo Kagaya and T. Soma, Phys. Status Solidi B **124**, 37 (1984).

[15] G. Roussos, H.-J. Schulz, and M. Thiede, J. Lumin. **31&32**, 409 (1984).

[16] J. H. Haanstra, in *International Conference on II-VI Semiconductor Compounds,* edited by D. G. Thomas (Benjamin, New York, 1967), p. 207.

[17] Georges Roussos, Ph.D. thesis, Technische Universität Berlin, 1983.

[18] G. A. Slack, S. Roberts, and F. S. Ham, Phys. Rev. **155**, 170 (1967).

[19] G. A. Slack, S. Roberts, and J. T. Vallin, Phys. Rev. **187**, 511 (1969).

[20] J. T. Vallin, Phys. Rev. B **2**, 2390 (1970).

[21] E. E. Vogel and J. Rivera-Iratchet, Phys. Rev. B **22**, 4511 (1980).

[22] G. Grebe and H.-J. Schulz, Z. Naturforsch. **29a**, 1803 (1974).

[23] J. Rivera-Iratchet, M. A. de Orúe, and E. E. Vogel, Phys. Rev. B **34**, 3992 (1986).

[24] E. E. Vogel, J. Rivera-Iratchet, and M. A. de Orúe, Phys. Rev. B **38**, 3556 (1988).

[25] M. K. Udo, M. Villeret, I. Mitkowski, A. J. Mayur, A. K. Ramdas, and S. Rodríguez, Phys. Rev. B **46**, 7459 (1992).